

A study of $\rho - \omega$ mixing in resonance chiral theory

Yun-Hua Chen,^{1,*} De-Liang Yao,^{2,†} and Han-Qing Zheng^{3,4,‡}

¹*School of Mathematics and Physics,*

University of Science and Technology Beijing, Beijing 100083, China

²*Instituto de Física Corpuscular (centro mixto CSIC-UV),*

Institutos de Investigación de Paterna, Apartado 22085, 46071, Valencia, Spain

³*Department of Physics and State Key Laboratory of Nuclear Physics and Technology,*

Peking University, Beijing 100871, China

⁴*Collaborative Innovation Center of Quantum Matter, Beijing 100871, China*

The strong and electromagnetic corrections to $\rho - \omega$ mixing are calculated using a SU(2) version of resonance chiral theory up to next-to-leading orders in $1/N_C$ expansion, respectively. Up to our accuracy, the effect of the momentum dependence of $\rho - \omega$ mixing is incorporated due to the inclusion of loop contributions. We analyze the impact of $\rho - \omega$ mixing on the pion vector form factor by performing numerical fit to the data extracted from $e^+e^- \rightarrow \pi^+\pi^-$ and $\tau \rightarrow \nu_\tau 2\pi$, while the decay width of $\omega \rightarrow \pi^+\pi^-$ is taken into account as a constraint. It is found that the momentum dependence is significant in a good description of the experimental data. In addition, based on the fitted values of the involved parameters, we analyze the decay width of $\omega \rightarrow \pi^+\pi^-$, which turns out to be highly dominated by the $\rho - \omega$ mixing effect.

I. INTRODUCTION

The study of $\rho - \omega$ mixing is a very interesting subject in hadron physics both theoretically and experimentally. The inclusion of $\rho - \omega$ mixing effect is crucial for a good description of the pion vector form factor in $e^+e^- \rightarrow \pi^+\pi^-$ process, which quantifies the hadronic vacuum polarization contribution to the anomalous magnetic moment of the muon. On the experimental side, several experimental collaborations, such as KLOE [1, 2] and BESIII [3], have recently launched measurements of the $e^+e^- \rightarrow \pi^+\pi^-$ with high statistics and high precision.

The $\rho - \omega$ mixing amplitude was assumed to be a constant or momentum-independent in the early stage of previous studies [4, 5]. The authors of Ref. [6] suspect the validity of the constant assumption and, based on a quark loop mechanism of $\rho - \omega$ mixing, they found that the mixing amplitude is significantly momentum-dependent. Since then, the use of various loop mechanisms for $\rho - \omega$ mixing is triggered in different models such as extended Nambu-Jona-Lasinio (NJL) model [7], the global color model [8], the hidden local symmetry model [9–11], and the chiral constituent quark model [12, 13].

In this work, we aim at studying $\rho - \omega$ mixing in a model independent way by invoking Resonance Chiral Theory (R χ T) [14]. It provides a reliable tool to study physics in the intermediate energy region [15–20]. The tree-level calculation of $\rho - \omega$ mixing in the framework of R χ T has been given in Refs. [21, 22], however, the tree-level mixing amplitude turns out to be momentum-independent. In order to implement the momentum de-

pendence, here we will calculate the one-loop contributions as shown in Fig. 1. The $\rho - \omega$ mixing can be induced either by strong isospin-violating or by electromagnetic effects. The former is proportional to the mass difference between the u, d quarks, i.e., $\Delta_{ud} = m_u - m_d$ and the latter is accompanied by the fine structure constant α . In the present study, only the mixing effects linear in Δ_{ud} or α are under our consideration. Apart from the overall factors Δ_{ud} or α , the large- N_C counting rule proposed in Ref. [23] is imposed to truncate our perturbative calculation. Specifically, our calculations are truncated at next-to-leading order in the $1/N_C$ expansion for the strong and electromagnetic contributions. The ultraviolet (UV) divergence from the loops is cancelled by introducing counterterms with sufficient derivatives and the involved couplings are assumed to be beyond the leading order in $1/N_C$ expansion as claimed in Ref. [24].

We assess the impact of momentum-dependent $\rho - \omega$ mixing amplitude on the pion vector form factor by fitting to the experimental data extracted from the $e^+e^- \rightarrow \pi^+\pi^-$ process and $\tau \rightarrow \nu_\tau 2\pi$ decay in the energy region of 650–850 MeV. Besides, the decay width of $\omega \rightarrow \pi^+\pi^-$ is implemented as a constraint in the fit. It is known that, provided isospin invariance holds, the isovector part of the pion form factor in the e^+e^- annihilation is related to the one in τ decays theoretically, via the conserved vector current assumption [25, 26]. Different effects of isospin breaking have been studied to describe the e^+e^- annihilation data and τ decays data simultaneously [26–34], such as the short distance and long distance corrections in the τ partial decay width to two pions, charged and neutral ρ mass and width difference, and $\rho - \omega$ mixing. In our study we will take into account all the above isospin breaking effects. Our fit result shows that the $\rho - \omega$ mixing amplitude is significantly momentum-dependent and its imaginary part is much smaller than real part. Based on the fitted values of the parameters, we also analyze the decay width of $\omega \rightarrow \pi^+\pi^-$ by including the effect of

*yhchen@ustb.edu.cn

†Corresponding author: deliang.yao@ific.uv.es

‡zhenghq@pku.edu.cn

the ρ - ω mixing. It is found that the decay width is dominated by the ρ - ω mixing effect while the contribution from the direct coupling of $\omega_I \rightarrow \pi^+\pi^-$ is negligible.

This paper is organized as follows. In Sec. II, we introduce the description of ρ - ω mixing. In Sec. III, we present the theoretical framework and elaborate on the calculation of the tree-level and loop contribution of ρ - ω mixing. In Sec. IV, the fit result is shown and the related phenomenology is discussed. A summary is given in Sec. V.

II. GENERIC DESCRIPTION OF ρ - ω MIXING

In the isospin basis $|I, I_3\rangle$, we define $|\rho_I\rangle \equiv |1, 0\rangle$ and $|\omega_I\rangle \equiv |0, 0\rangle$ for convenience. The mixing between the isospin states of $|\rho_I\rangle$ and $|\omega_I\rangle$ can be implemented by considering the self-energy matrix

$$\Pi_{\mu\nu} = T_{\mu\nu} \begin{pmatrix} \Pi_{\rho\rho}(s) & \Pi_{\rho\omega}(s) \\ \Pi_{\rho\omega}(s) & \Pi_{\omega\omega}(s) \end{pmatrix}, \quad (1)$$

with $T_{\mu\nu} \equiv g_{\mu\nu} - \frac{p^\mu p^\nu}{p^2}$ and $s \equiv p^2$. The off-diagonal matrix element $\Pi_{\rho\omega}(s)$ is non-zero, e.g., due to isospin-breaking effect, and it therefore carries the information of ρ - ω mixing. Subsequently, the dressed propagator has the form [35]

$$D_{\mu\nu} = g_{\mu\nu} \begin{pmatrix} 1/s_\rho & \frac{\Pi_{\rho\omega}(s)}{s_\rho s_\omega} \\ \frac{\Pi_{\rho\omega}(s)}{s_\rho s_\omega} & 1/s_\omega \end{pmatrix} \equiv g_{\mu\nu} D^I(s), \quad (2)$$

where the abbreviations s_ρ and s_ω are defined by

$$\begin{aligned} s_\rho &\equiv s - \Pi_{\rho\rho}(s) - m_\rho^2, \\ s_\omega &\equiv s - \Pi_{\omega\omega}(s) - m_\omega^2. \end{aligned} \quad (3)$$

In above the vector-current conservation has been used to eliminate the longitudinal part proportional to p_μ . Furthermore, we have also neglected terms of $\Pi_{\rho\omega}^2(s)$, since they correspond to contributions at two-loop order and are beyond our accuracy. m_ρ and m_ω are bare masses of the ρ and ω mesons, respectively.

The ρ - ω mixing, i.e., mixing between the physical states of ρ^0 and ω , is obtainable by introducing the following relation

$$\begin{pmatrix} \rho^0 \\ \omega \end{pmatrix} = C \begin{pmatrix} \rho_I \\ \omega_I \end{pmatrix}, \quad C = \begin{pmatrix} 1 & -\epsilon_1 \\ \epsilon_2 & 1 \end{pmatrix} \quad (4)$$

with ϵ being the mixing parameter. The matrix of dressed propagators corresponding to physical states is

diagonal. Moreover, it can be connected to the matrix $D^I(s)$ in Eq. (2) through

$$\begin{pmatrix} 1/s_\rho & 0 \\ 0 & 1/s_\omega \end{pmatrix} = C \begin{pmatrix} 1/s_\rho & \Pi_{\rho\omega}/s_\rho s_\omega \\ \Pi_{\rho\omega}/s_\rho s_\omega & 1/s_\omega \end{pmatrix} C^{-1}. \quad (5)$$

Solving the above equation and neglecting higher-order terms of $\mathcal{O}(\epsilon^2)$ and $\epsilon \Pi_{\rho\omega}$, one obtains:

$$\epsilon_1 = \frac{\Pi_{\rho\omega}(M_\omega^2)}{s_\rho - s_\omega}, \quad \epsilon_2 = \frac{\Pi_{\rho\omega}(M_\rho^2)}{s_\rho - s_\omega}. \quad (6)$$

The two mixing parameters should be just different with each other slightly, see Ref. [35] for more details.

III. CALCULATIONS IN RESONANCE CHIRAL THEORY

In this section we will calculate the mixing amplitude $\Pi_{\rho\omega}(s)$ using R χ T so as to study its momentum dependence. The information of ρ - ω mixing is encoded in the off-diagonal element of the self-energy matrix, which can be decomposed as

$$\Pi_{\rho\omega}(s) = \Delta_{ud} S_{\rho\omega}(s) + 4\pi\alpha E_{\rho\omega}(s), \quad (7)$$

where $\Delta_{ud} = m_u - m_d$ is the mass difference between u, d quarks, and α denotes the fine-structure constant. In above, $S_{\rho\omega}(s)$ and $E_{\rho\omega}(s)$ stand for the structure functions of strong and electromagnetic interactions, respectively. In the present work, the diagrams in Fig. 1 are needed for a calculation in R χ T up to NLO in $1/N_C$ expansion. As will be seen below, the LO contributions of $S_{\rho\omega}(s)$ and $E_{\rho\omega}(s)$ are different: the former starts at $\mathcal{O}(N_C^0)$ while the latter does at $\mathcal{O}(N_C^1)$. Therefore, their corresponding NLO contributions are of $\mathcal{O}(N_C^{-1})$ and $\mathcal{O}(N_C^0)$, respectively. In what follows, all the diagrams in Fig. 1 will be calculated by using effective Lagrangians constructed in the framework of R χ T.

A. Resonance chiral theory and Tree-level amplitudes

In R χ T, the vector resonances are described in terms of antisymmetry tensor fields with the normalization

$$\langle 0 | V_{\mu\nu} | V, p \rangle = i M_V^{-1} \{ p_\mu \epsilon_\nu(p) - p_\nu \epsilon_\mu(p) \}, \quad (8)$$

with ϵ_μ being the polarization vector. The kinetic Lagrangian of vector resonances takes the form [14]

$$\mathcal{L}_{kin}(V) = -\frac{1}{2} \langle \nabla^\lambda V_{\lambda\mu} \nabla_\nu V^{\nu\mu} - \frac{M_V^2}{2} V_{\mu\nu} V^{\mu\nu} \rangle, \quad (9)$$

where M_V is the mass of the vector resonances in the chiral limit. Here the vector mesons are collected in a 2×2 matrix

$$V_{\mu\nu} = \begin{pmatrix} \frac{1}{\sqrt{2}}\rho^0 + \frac{1}{\sqrt{2}}\omega & \rho^+ \\ \rho^- & -\frac{1}{\sqrt{2}}\rho^0 + \frac{1}{\sqrt{2}}\omega \end{pmatrix}_{\mu\nu}. \quad (10)$$

¹ Without loss of generality, here we use the Proca formalism for the vector fields and $T_{\mu\nu}$ is the transverse projector. In the antisymmetric tensor formalism, the corresponding transverse projector is $\Omega_{\mu\nu\rho\sigma}^T = \frac{1}{2p^2} [(g_{\mu\rho}p_\nu p_\sigma - g_{\rho\nu}p_\mu p_\sigma) - (\rho \leftrightarrow \sigma)]$.

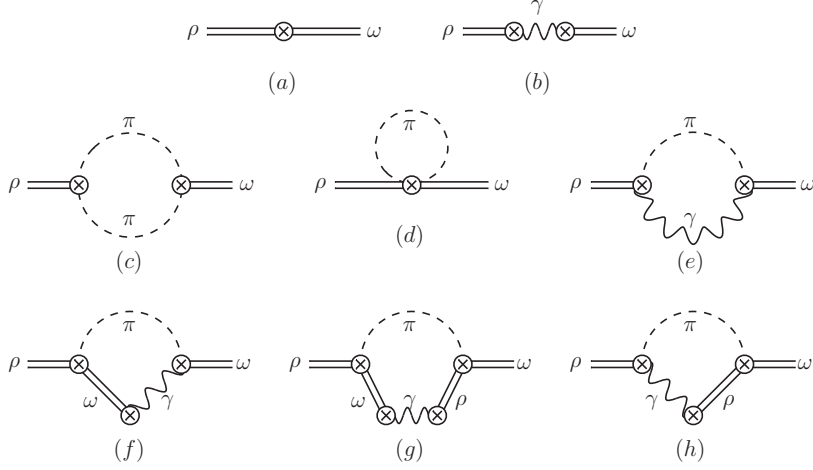


FIG. 1: Feynman diagrams contributing to $\rho - \omega$ mixing.

Besides, the covariant derivative and chiral connection are defined by

$$\begin{aligned}\nabla_\mu V &= \partial_\mu V + [\Gamma_\mu, V], \\ \Gamma_\mu &= \frac{1}{2}\{u^+(\partial_\mu - ir_\mu)u + u(\partial_\mu - il_\mu)u^+\}.\end{aligned}\quad (11)$$

The Goldstone bosons originating from the spontaneous breaking of the $SU(2)_L \times SU(2)_R$ chiral symmetry are nonlinearly parametrized as

$$u = \exp\left\{i\frac{\Phi}{\sqrt{2}F}\right\}, \quad \Phi = \begin{pmatrix} \frac{1}{\sqrt{2}}\pi^0 & \pi^+ \\ \pi^- & -\frac{1}{\sqrt{2}}\pi^0 \end{pmatrix}, \quad (12)$$

with F being the pion decay constant.

In the isospin limit, the standard Lagrangian describing the interactions between $V_{\mu\nu}$ and Goldstone bosons or electromagnetic fields are given by

$$\mathcal{L}_2(V) = \frac{F_V}{2\sqrt{2}}\langle V_{\mu\nu}f_+^{\mu\nu}\rangle + \frac{iG_V}{\sqrt{2}}\langle V_{\mu\nu}u^\mu u^\nu\rangle, \quad (13)$$

with the relevant building blocks defined by

$$\begin{aligned}f_\pm^{\mu\nu} &= uF_L^{\mu\nu}u^\pm \pm u^\pm F_R^{\mu\nu}u, \\ u_\mu &= i[u^+(\partial_\mu - ir_\mu)u - u(\partial_\mu - il_\mu)u^+].\end{aligned}\quad (14)$$

Here $F_{L,R}^{\mu\nu}$ are field strength tensors composed of the left and right external sources l_μ and r_μ , and F_V, G_V are real couplings.

The LO isospin-breaking effect is introduced by the Lagrangian

$$\mathcal{L}_2^{\rho\omega} = v_8\langle V_{\mu\nu}V^{\mu\nu}\chi_+\rangle, \quad (15)$$

with $\chi_+ = u^+\chi u^+ + u\chi^+u$ and $\chi = 2B_0(s + ip)$. Here v_8 is an unknown coupling constant. However, it can be determined by considering the mass relations of the vector mesons at $O(p^2)$ in terms of the quark counting rule [21], which leads to: $v_8 = 1/8$.

With the above preparations, one is now able to calculate the tree amplitudes. The tree-level strong contribution, corresponding to diagram (a) in Fig. 1, turns out to be

$$S_{\rho\omega}^{(a)} = 2M_\rho, \quad (16)$$

which is counted as $O(N_C^0)$, since $M_\rho \sim O(N_C^0)$. The tree-level electromagnetic contribution is from diagram (b) in Fig. 1 and the amplitude can be obtained by using the Lagrangian in Eq. (13):

$$E_{\rho\omega}^{(b)} = \frac{F_\rho F_\omega}{3}, \quad (17)$$

with the N_C -counting order being $O(N_C^1)$ due to $F_\rho \sim F_\omega \sim \sqrt{N_C}$. As mentioned in the beginning of this section, the leading-order strong and electromagnetic contributions indeed start at different orders in $1/N_C$ expansion.

B. Loop contributions

The relevant loop diagrams contributing up to our accuracy are shown in the second and third lines of Fig. 1. Diagrams (c) and (d) contribute to the strong correction at $O(N_C^{-1})$, which are next-to-leading order compared to diagram (a). Likewise, with respect to diagram (b), diagrams (e)-(h) lead to electromagnetic corrections at next-to-leading order, i.e. $O(N_C^0)$. In our calculation below, the necessary isospin-breaking vertices are constructed based on the basic chiral building blocks taken from χ PT [36] and $R\chi$ T [14].

1. Diagram (c): $\pi\pi$ loop

The vertex of $\rho_I \rightarrow \pi^+\pi^-$ can be read from the Lagrangian in Eq. (13). For the isospin-violating vertex of

$\omega_I \rightarrow \pi^+ \pi^-$, we construct the following Lagrangian

$$\begin{aligned}\mathcal{L}_{\omega_I \rightarrow \pi^+ \pi^-} &= a_1 i \langle V_{\mu\nu} \{ \chi_+, u^\mu u^\nu \} \rangle + a_2 i \langle V_{\mu\nu} u^\mu \chi_+ u^\nu \rangle \\ &= (a_1 - \frac{1}{2}a_2) \frac{8\sqrt{2}B_0 i}{F^2} \Delta_{ud} \omega_{\alpha\beta} \pi^+ \pi^- .\end{aligned}\quad (18)$$

For convenience, we define the combination $a \equiv a_1 - \frac{1}{2}a_2$. The $\pi\pi$ -loop contribution can be obtained by calculating the integral

$$\begin{aligned}i\Pi_{\rho\omega} \epsilon_{\rho\mu} \epsilon_\omega^\mu &= -\frac{16\sqrt{2}G_V B_0 a (m_u - m_d) p^2}{F^4} \epsilon_{\rho\mu} \epsilon_{\omega\nu} \\ &\times \int \frac{d^n k}{(2\pi)^n} \frac{k^\mu k^\nu}{[k^2 - m_\pi^2][(p-k)^2 - m_\pi^2]} \quad (19)\end{aligned}$$

where p and k denote the momenta of the external vector meson and either of the exchanged pions, respectively. After integrating, the structure function can be extracted, which reads

$$\begin{aligned}S_{\rho\omega}^{(c)} &= \frac{\sqrt{2}G_V B_0 a}{12F^4 \pi^2} p^4 \left\{ \left(1 - \frac{6m_\pi^2}{p^2}\right) (\lambda_\infty - \ln \frac{m_\pi^2}{\mu^2}) \right. \\ &\quad \left. + \frac{5}{3} - \frac{8m_\pi^2}{p^2} + \sigma^3 \ln \left(\frac{\sigma+1}{\sigma-1}\right) \right\}, \quad (20)\end{aligned}$$

where $\sigma \equiv \sqrt{1 - 4m_\pi^2/p^2}$ and $\lambda_\infty \equiv \frac{1}{\epsilon} - \gamma_E + 1 + \ln 4\pi$ with $\epsilon = 2 - \frac{d}{2}$ and γ_E being the Euler constant.

2. Diagram (d): π -tadpole loop

According to the Lorentz, P and C invariances, the Lagrangian corresponding to the interaction of $\omega_I \rho_I \pi \pi$ can be written down as follows:

$$\begin{aligned}\mathcal{L}_{\omega_I \rho_I P P} &= b_1 \langle V_{\mu\nu} V^{\mu\nu} (u^\alpha u_\alpha \chi_+ + \chi_+ u^\alpha u_\alpha) \rangle \\ &+ b_2 \langle V_{\mu\nu} V^{\mu\nu} u^\alpha \chi_+ u_\alpha \rangle + b_3 \langle V_{\mu\nu} \chi_+ V^{\mu\nu} u^\alpha u_\alpha \rangle \\ &+ b_4 \langle V_{\mu\nu} u^\alpha V^{\mu\nu} (\chi_+ u_\alpha + u_\alpha \chi_+) \rangle \\ &+ b_5 \langle V_{\mu\alpha} V^{\nu\alpha} u^\mu u_\nu \chi_+ + V^{\nu\alpha} V_{\mu\alpha} \chi_+ u_\nu u^\mu \rangle \\ &+ b_6 \langle V_{\mu\alpha} V^{\nu\alpha} u^\mu \chi_+ u_\nu \rangle + b_7 \langle V_{\mu\alpha} \chi_+ V^{\nu\alpha} u^\mu u_\nu \rangle \\ &+ b_8 \langle V_{\mu\alpha} V^{\nu\alpha} u_\nu u^\mu \chi_+ + V^{\nu\alpha} V_{\mu\alpha} \chi_+ u^\mu u_\nu \rangle \\ &+ b_9 \langle V_{\mu\alpha} V^{\nu\alpha} u_\nu \chi_+ u^\mu \rangle + b_{10} \langle V_{\mu\alpha} \chi_+ V^{\nu\alpha} u_\nu u^\mu \rangle \\ &+ b_{11} \langle V_{\mu\alpha} u^\alpha V^{\mu\beta} u_\beta \chi_+ + V^{\mu\beta} u^\alpha V_{\mu\alpha} \chi_+ u_\beta \rangle \\ &+ b_{12} \langle V_{\mu\alpha} u^\alpha V^{\mu\beta} \chi_+ u_\beta + V^{\mu\beta} u^\alpha V_{\mu\alpha} u_\beta \chi_+ \rangle \\ &+ b_{13} \langle V_{\mu\alpha} u_\beta V^{\mu\beta} u^\alpha \chi_+ + V^{\mu\beta} u_\beta V_{\mu\alpha} \chi_+ u^\alpha \rangle \\ &+ b_{14} \langle V_{\mu\alpha} u_\beta V^{\mu\beta} \chi_+ u^\alpha + V^{\mu\beta} u_\beta V_{\mu\alpha} u^\alpha \chi_+ \rangle \\ &+ g_1 i \langle V_{\mu\nu} V^{\mu\nu} (u^\alpha \nabla_\alpha \chi_- + \nabla_\alpha \chi_- u^\alpha) \rangle \\ &+ g_2 i \langle V_{\mu\nu} u^\alpha V^{\mu\nu} \nabla_\alpha \chi_- \rangle \\ &+ g_3 i \langle V_{\mu\beta} V^{\mu\alpha} u^\beta \nabla_\alpha \chi_- + V^{\mu\alpha} V_{\mu\beta} \nabla_\alpha \chi_- u^\beta \rangle \\ &+ g_4 i \langle V_{\mu\beta} V^{\mu\alpha} \nabla_\alpha \chi_- u^\beta + V^{\mu\alpha} V_{\mu\beta} u^\beta \nabla_\alpha \chi_- \rangle \\ &+ g_5 i \langle V_{\mu\beta} u^\beta V^{\mu\alpha} \nabla_\alpha \chi_- + V^{\mu\alpha} u^\beta V_{\mu\beta} \nabla_\alpha \chi_- \rangle \\ &+ v_8 \langle V_{\mu\nu} V^{\mu\nu} \chi_+ \rangle. \quad (21)\end{aligned}$$

Note that the $v_8 \langle V_{\mu\nu} V^{\mu\nu} \chi_+ \rangle$ term, which contributes to the contact interaction of ρ - ω mixing, also yields $\omega_I \rho_I \pi \pi$ vertex. Though in Eq. (21) there are many terms with a large number of free couplings, the final result only depends on combinations of these couplings. For simplicity, the following two combinations are necessary, i.e.,

$$\begin{aligned}h_1 &\equiv 6b_1 - b_2 + 3b_3 + b_4 - 2g_1 - g_2, \\ h_2 &\equiv 4b_5 - b_6 + 3b_7 + 4b_8 - b_9 + 3b_{10} + 2b_{11} + 2b_{12} \\ &\quad + 2b_{13} + 2b_{14} - 2g_3 - 2g_4 - 2g_5. \quad (22)\end{aligned}$$

Furthermore, one can neglect the mass difference between the charged and neutral pions in the internal lines of loops, since the resultant difference is of higher orders beyond our consideration. As a result, the expanded form of Lagrangian (21) can be reduced simply to

$$\begin{aligned}\mathcal{L}_{\omega_I \rho_I \pi \pi} &= \frac{4B_0}{F^2} h_1 (m_u - m_d) \rho_{I\mu\nu} \omega^{\mu\nu} \pi_\alpha \pi^\alpha \\ &- \frac{2B_0}{F^2} v_8 (m_u - m_d) \rho_{I\mu\nu} \omega^{\mu\nu} \pi^2 \\ &+ \frac{4B_0}{F^2} h_2 (m_u - m_d) \rho_{I\mu\alpha} \omega^{\nu\alpha} \pi_\mu \pi^\nu. \quad (23)\end{aligned}$$

With the above Lagrangian, the π -tadpole contribution to the ρ - ω mixing can be derived:

$$\begin{aligned}i\Pi_{\rho\omega} \epsilon_{\rho\mu} \epsilon_\omega^\mu &= \frac{4iB_0}{F^2} h_1 (m_u - m_d) \epsilon_{\rho\mu} \epsilon_\omega^\mu \int \frac{d^n k}{(2\pi)^n} \frac{2ik^2}{k^2 - m_\pi^2} \\ &+ \frac{4iB_0}{F^2 p^2} h_2 (m_u - m_d) (p_\mu p_\nu \epsilon_{\rho\alpha} \epsilon_\omega^\alpha + p^2 \epsilon_{\rho\mu} \epsilon_{\omega\mu}) \\ &\times \int \frac{d^n k}{(2\pi)^n} \frac{ik^\mu k^\nu}{k^2 - m_\pi^2} - i \frac{32B_0}{F^2} v_8 (m_u - m_d) \\ &\times \epsilon_{\rho\mu} \epsilon_\omega^\mu \int \frac{d^n k}{(2\pi)^n} \frac{i}{k^2 - m_\pi^2}. \quad (24)\end{aligned}$$

Eventually, the explicit expression of the strong structure function has the form of

$$\begin{aligned}S_{\rho\omega}^{(d)} &= -\frac{m_\pi^2 B_0}{8\pi^2 F^2} \left\{ (-16v_8 + 4h_1 m_\pi^2 + h_2 m_\pi^2) \right. \\ &\quad \left. \times (\lambda_\infty - \ln \frac{m_\pi^2}{\mu^2}) + \frac{h_2}{2} \right\}. \quad (25)\end{aligned}$$

3. Diagrams (e)-(h): $\pi^0 \gamma$ loops

In the loop diagrams (e)-(h), there are two types of vertices. The coupling of vector meson (V) as well as vector external source (J) to pseudoscalar (P) is labeled by VJP vertex for short. The interaction of two vector mesons and one pseudoscalar is called VVP vertex. The operators of VJP type are given in Ref. [37]:

$$\begin{aligned}\mathcal{L}_{VJP} &= \frac{c_1}{M_V} \epsilon_{\mu\nu\rho\sigma} \langle \{ V^{\mu\nu}, f_+^{\rho\alpha} \} \nabla_\alpha u^\sigma \rangle \\ &+ \frac{c_2}{M_V} \epsilon_{\mu\nu\rho\sigma} \langle \{ V^{\mu\alpha}, f_+^{\rho\sigma} \} \nabla_\alpha u^\nu \rangle\end{aligned}$$

$$\begin{aligned}
& + \frac{ic_3}{M_V} \epsilon_{\mu\nu\rho\sigma} \langle \{V^{\mu\nu}, f_+^{\rho\sigma}\} \chi_- \rangle \\
& + \frac{ic_4}{M_V} \epsilon_{\mu\nu\rho\sigma} \langle V^{\mu\nu} [f_-^{\rho\sigma}, \chi_+] \rangle \\
& + \frac{c_5}{M_V} \epsilon_{\mu\nu\rho\sigma} \langle \{ \nabla_\alpha V^{\mu\nu}, f_+^{\rho\alpha} \} u^\sigma \rangle \\
& + \frac{c_6}{M_V} \epsilon_{\mu\nu\rho\sigma} \langle \{ \nabla_\alpha V^{\mu\alpha}, f_+^{\rho\sigma} \} u^\nu \rangle \\
& + \frac{c_7}{M_V} \epsilon_{\mu\nu\rho\sigma} \langle \{ \nabla^\sigma V^{\mu\nu}, f_+^{\rho\alpha} \} u_\alpha \rangle, \quad (26)
\end{aligned}$$

and the ones of VVP type are

$$\begin{aligned}
\mathcal{L}_{VVP} = & d_1 \epsilon_{\mu\nu\rho\sigma} \langle \{V^{\mu\nu}, V^{\rho\alpha}\} \nabla_\alpha u^\sigma \rangle \\
& + id_2 \epsilon_{\mu\nu\rho\sigma} \langle \{V^{\mu\nu}, V^{\rho\sigma}\} \chi_- \rangle \\
& + d_3 \epsilon_{\mu\nu\rho\sigma} \langle \{ \nabla_\alpha V^{\mu\nu}, V^{\rho\alpha} \} u^\sigma \rangle \\
& + d_4 \epsilon_{\mu\nu\rho\sigma} \langle \{ \nabla^\sigma V^{\mu\nu}, V^{\rho\alpha} \} u_\alpha \rangle. \quad (27)
\end{aligned}$$

The involved couplings or their combinations can be estimated by matching the leading operator product expansion of $\langle VVP \rangle$ Green function to the result calculated within $R\chi T$. Such a procedure leads to high energy constraints on the resonance couplings as follows [37]:

$$\begin{aligned}
4c_3 + c_1 &= 0, \\
c_1 - c_2 + c_5 &= 0, \\
c_5 - c_6 &= \frac{N_c}{64\pi^2} \frac{M_V}{\sqrt{2}F_V}, \\
d_1 + 8d_2 &= -\frac{N_c}{64\pi^2} \frac{M_V^2}{F_V^2} + \frac{F^2}{4F_V^2}, \\
d_3 &= -\frac{N_c}{64\pi^2} \frac{M_V^2}{F_V^2} + \frac{F^2}{8F_V^2}. \quad (28)
\end{aligned}$$

The mass of vectors in the chiral limit, M_V , can be estimated by the mass of $\rho(770)$ meson [38].

The loops diagrams (e)-(h) can be calculated simultaneously if the effective vertices of $\rho^* \rightarrow \pi^* \gamma^*$ and $\omega^* \rightarrow \pi^* \gamma^*$ are used, where a "*" stands for an off-shell particle. The explicit expression for $\rho^* \rightarrow \pi^* \gamma^*$ reads

$$\begin{aligned}
i\mathcal{V}_{\text{eff}}^{\rho^* \pi^* \gamma^*} = & i\epsilon_{\mu\nu\alpha\beta} k^\mu p^\nu \epsilon_{\rho^*}^\alpha \epsilon_{\gamma^*}^\beta \frac{4\sqrt{2}eB_0}{3M_\rho M_V F} [c_1(p-k) \cdot k \\
& - c_2 p \cdot (p-k) - 4c_3 m_\pi^2 - c_5 p \cdot k + c_6 p^2] \\
& + i\epsilon_{\mu\nu\alpha\beta} k^\mu p^\nu \epsilon_{\rho^*}^\alpha \epsilon_{\gamma^*}^\beta \frac{4F_V e B_0}{3M_\rho F (M_\omega^2 - k^2)} \\
& \times [d_1(p-k)^2 + 8d_2 m_\pi^2 + 2d_3 p \cdot k], \quad (29)
\end{aligned}$$

where p and k denote the momentum of the vector meson and the photon, respectively. Analogically, for $\omega^* \rightarrow \pi^* \gamma^*$, one has

$$\begin{aligned}
i\mathcal{V}_{\text{eff}}^{\omega^* \pi^* \gamma^*} = & i\epsilon_{\mu\nu\alpha\beta} k^\mu p^\nu \epsilon_{\omega^*}^\alpha \epsilon_{\gamma^*}^\beta \frac{4\sqrt{2}eB_0}{M_\omega M_V F} [c_1(p-k) \cdot k \\
& - c_2 p \cdot (p-k) - 4c_3 m_\pi^2 - c_5 p \cdot k + c_6 p^2] \\
& + i\epsilon_{\mu\nu\alpha\beta} k^\mu p^\nu \epsilon_{\omega^*}^\alpha \epsilon_{\gamma^*}^\beta \frac{4F_V e B_0}{M_\omega F (M_\rho^2 - k^2)}
\end{aligned}$$

$$\times [d_1(p-k)^2 + 8d_2 m_\pi^2 + 2d_3 p \cdot k]. \quad (30)$$

It should be stressed that there are two terms in each effective vertex. One corresponds to the case that the virtual photon is coupled to the VP system directly, while the other to the case that it is interacted through an intermediate vector meson. Note also that, throughout this work we only account for the corrections proportional either to Δ_{ud} or $4\pi\alpha$, which implies the calculation of electromagnetic contribution can be carried out in the isospin limit, i.e., $m_u = m_d$.

With the help of the effective vertices, the $\pi\gamma$ loop contribution, i.e., the sum of the loops diagrams (e)-(h), can be expressed as:

$$\begin{aligned}
i\Pi_{\rho\omega} \epsilon_{\rho\mu} \epsilon_\omega^\mu = & \frac{1}{p^2} \int \frac{d^n k}{(2\pi)^n} \frac{-i}{k^2} \frac{i}{(p-k)^2 - m_\pi^2} \\
& \times [(k \cdot p)^2 \epsilon_\rho^\mu \epsilon_{\omega\mu} - k^2 p^2 \epsilon_\rho^\mu \epsilon_{\omega\mu} + p^2 k \cdot \epsilon_\rho k \cdot \epsilon_\omega] \\
& \times \left\{ \frac{-32e^2}{3M_V^2 F^2} [c_1(p-k) \cdot k - c_2(p-k) \cdot p \right. \\
& \quad \left. - 4c_3 m_\pi^2 - c_5 p \cdot k + c_6 p^2]^2 \right. \\
& \quad \left. - \frac{16\sqrt{2}F_V e^2}{3M_V F^2} \left[\frac{1}{M_\omega^2 - k^2} + \frac{1}{M_\rho^2 - k^2} \right] \right. \\
& \quad \times [d_1(p-k)^2 + 8d_2 m_\pi^2 + 2d_3 p \cdot k] \\
& \quad \times [c_1(p-k) \cdot k - c_2(p-k) \cdot p - 4c_3 m_\pi^2 \\
& \quad \left. - c_5 p \cdot k + c_6 p^2] - \frac{16F_V^2 e^2}{3F^2 (M_\rho^2 - k^2)(M_\omega^2 - k^2)} \right. \\
& \quad \left. \times [d_1(p-k)^2 + 8d_2 m_\pi^2 + 2d_3 p \cdot k]^2 \right\}.
\end{aligned}$$

The further calculation is straightforward but the result of the extracted electromagnetic structure function $E_{\rho\omega}^{\pi\gamma} \equiv E_{\rho\omega}^{(e)} + E_{\rho\omega}^{(f)} + E_{\rho\omega}^{(g)} + E_{\rho\omega}^{(h)}$ is too lengthy to be shown here. It is worthy noting that in our numerical computation we will use the high energy constraints in Eq. (28) together with the fitted parameters given in Ref. [18], therefore, all the parameters involved in $E_{\rho\omega}^{\pi\gamma}$ are known.

4. counterterms and renormalized amplitude

Up to now, the total contribution of $\rho - \omega$ mixing can be expressed as

$$\Pi_{\rho\omega} = \Delta_{ud} [S_{\rho\omega}^{(a)} + S_{\rho\omega}^{(c)} + S_{\rho\omega}^{(d)}] + 4\pi\alpha [E_{\rho\omega}^{(b)} + E_{\rho\omega}^{\pi\gamma}],$$

which is still unrenormalized. The resonance chiral theory is unrenormalizable in the sense that the amplitude has to be renormalized order by order with increasing number of counterterms when the accuracy of the calculation is improved. In our case, the tree amplitudes, $S_{\rho\omega}^{(a)}$ and $E_{\rho\omega}^{(b)}$, can only absorb the ultraviolet divergence proportional to p^0 . In order to cancel the $O(p^2)$, $O(p^4)$ and $O(p^6)$ stemming from the loop contribution $S_{\rho\omega}^{(c)}$ and

$E_{\rho\omega}^{\pi\gamma}$, additional counterterms are needed. For this purpose, we construct

$$\begin{aligned}\mathcal{L}_{ct} = & Y_A \langle V_{\mu\nu} V^{\mu\nu} \chi_+ \rangle - \frac{1}{2} Y_B \langle \nabla^\lambda V_{\lambda\mu} \nabla_\nu V^{\nu\mu} \chi_+ \rangle \\ & + \frac{Y_{C_1}}{2} \langle \nabla^2 V^{\mu\nu} \{ \chi_+, \{ \nabla_\nu, \nabla^\sigma \} V_{\mu\sigma} \} \rangle \\ & + \frac{Y_{C_2}}{4} \langle \{ \nabla_\nu, \nabla_\alpha \} V^{\mu\nu} \{ \chi_+, \{ \nabla^\sigma, \nabla^\alpha \} V_{\mu\sigma} \} \rangle \\ & + \frac{Y_{C_3}}{4} \langle \{ \nabla^\sigma, \nabla^\alpha \} V^{\mu\nu} \{ \chi_+, \{ \nabla_\nu, \nabla_\alpha \} V_{\mu\sigma} \} \rangle \\ & + \frac{Z_A F_V}{2\sqrt{2}} \langle V_{\mu\nu} f_+^{\mu\nu} \rangle + \frac{Z_B F_V}{2\sqrt{2}} \langle V_{\mu\nu} \nabla^2 f_+^{\mu\nu} \rangle \\ & + \frac{Z_C F_V}{2\sqrt{2}} \langle V_{\mu\nu} \nabla^4 f_+^{\mu\nu} \rangle + \frac{Z_D F_V}{2\sqrt{2}} \langle V_{\mu\nu} \nabla^6 f_+^{\mu\nu} \rangle.\end{aligned}\quad (32)$$

We adopt the $\overline{\text{MS}} - 1$ subtraction scheme and absorb the divergent pieces proportional to λ_∞ by the bare couplings in the counterterms. Consequently, the remanent finite pieces of counterterms can be written as:

$$\Pi_{\rho\omega}^{ct} = X_W^r p^6 + X_Z^r p^4 + X_R^r p^2, \quad (33)$$

with

$$\begin{aligned}X_W^r &\equiv \frac{8\pi\alpha F_\rho F_\omega}{3} (Z_D^r + Z_B^r Z_C^r), \\ X_Z^r &\equiv \frac{4\pi\alpha F_\rho F_\omega}{3} (2Z_C^r + Z_B^r{}^2) \\ &\quad + 16M_\rho(m_u - m_d)(Y_{C_1}^r + Y_{C_2}^r + Y_{C_3}^r), \\ X_R^r &\equiv \frac{8\pi\alpha F_\rho F_\omega}{3} Z_B^r - 4M_\rho(m_u - m_d)Y_B^r.\end{aligned}\quad (34)$$

In summary, the UV-renormalized mixing amplitude reads

$$\begin{aligned}\Pi_{\rho\omega}^r(p^2) = & 2M_\rho(m_u - m_d) + \frac{4\pi\alpha F_\rho F_\omega}{3} \\ & + \frac{\sqrt{2}G_V B_0 a}{12F^4\pi^2} (m_u - m_d) p^4 \left\{ \left(\frac{6m_\pi^2}{p^2} - 1 \right) \ln \frac{m_\pi^2}{\mu^2} \right. \\ & + \frac{5}{3} - \frac{8m_\pi^2}{p^2} + \sigma^3 \ln \left(\frac{\sigma + 1}{\sigma - 1} \right) \left. \right\} \frac{m_\pi^2 B_0}{8\pi^2 F^2} (m_u - m_d) \\ & \times \left\{ (-16v_8 + 4h_1 m_\pi^2 + h_2 m_\pi^2) \ln \frac{m_\pi^2}{\mu^2} - \frac{h_2}{2} \right\} \\ & + \overline{E}_{\rho\omega}^{\pi\gamma}(p^2) + X_W^r p^6 + X_Z^r p^4 + X_R^r p^2,\end{aligned}\quad (35)$$

where a bar indicates the divergences are subtracted. As discussed in Ref. [35], there is an important constraint on the mixing amplitude, namely, it should vanish as $p^2 \rightarrow 0$. Thus the final expression of the renormalized mixing amplitude should be

$$\Pi_{\rho\omega}(p^2) = \Pi_{\rho\omega}^r(p^2) - \Pi_{\rho\omega}^r(0), \quad (36)$$

where an additional finite shift is imposed so as to guarantee that the constraint $\Pi_{\rho\omega}(0) = 0$ is satisfied.

In our numerical computation, the scale μ will be set to M_ρ and we use $(m_u - m_d) = -2.49$ MeV provided

by particle data group (PDG) [39]. Furthermore, we can define

$$f_4 \equiv \frac{m_\pi^2 B_0}{8\pi^2 F^2} (m_u - m_d) \left\{ (-16v_8 + 4h_1 m_\pi^2 + h_2 m_\pi^2) \ln \frac{m_\pi^2}{\mu^2} - \frac{h_2}{2} \right\}, \quad (37)$$

and in principle the unknown parameters in Eq. (35) are a , f_4 , X_W^r , X_Z^r and X_R^r .

IV. THE EFFECT OF $\rho - \omega$ MIXING ON PION VECTOR FORM FACTOR

The mass and width of ρ meson are conventionally determined by fitting to the data of $e^+e^- \rightarrow \pi^+\pi^-$ and $\tau \rightarrow \nu_\tau 2\pi$ [39], where various mechanisms are introduced to describe the $\rho - \omega$ mixing effect. To avoid intervening by their $\rho - \omega$ mixing mechanisms, we do not employ their extracted values for the mass and width, rather, we set the mass M_ρ , the relevant couplings G_ρ and F_ρ to be free parameters in our fit. As for the width, a energy-dependent form will be imposed, which is supposed to be dominated by the two π decay channel [40]:

$$\Gamma_\rho(s) = \frac{sM_\rho}{96\pi F^2} (1 - 4m_\pi^2/s)^{\frac{3}{2}}. \quad (38)$$

For the narrow-width resonance ω , we take $M_\omega = 782.65$ MeV and $\Gamma_\omega = 8.49$ MeV from PDG [39]. The physical coupling F_ω can be extracted from the decay width of $\omega \rightarrow e^+e^-$. Using the Lagrangian $\frac{F_V}{2\sqrt{2}} \langle V_{\mu\nu} f_+^{\mu\nu} \rangle$, one can derive the decay width

$$\Gamma_\omega^{e^+e^-} = \frac{4\alpha^2 \pi F_\omega^2 (2m_e^2 + M_\omega^2) \sqrt{M_\omega^2 - 4m_e^2}}{27M_\omega^4}, \quad (39)$$

and get $F_\omega \simeq 138$ MeV. With the decay widths given above, s_ρ and s_ω in Eq. (3) now can be rewritten as

$$\begin{aligned}s_\rho &\simeq s - M_\rho^2 + iM_\rho\Gamma_\rho(s), \\ s_\omega &\simeq s - M_\omega^2 + iM_\omega\Gamma_\omega.\end{aligned}\quad (40)$$

The experimental data considered in this work are the pion form factor $F_\pi(p^2)$ of the $e^+e^- \rightarrow \pi^+\pi^-$ process [1-3, 41-45] and $\tau \rightarrow \nu_\tau 2\pi$ decay [25, 46] in the energy region of 650~850 MeV, and the decay width of $\omega \rightarrow \pi^+\pi^-$ [39].

The Feynman amplitude for the process $\gamma^* \rightarrow \pi^+\pi^-$, proceeding via virtual intermediate hadrons, i.e., ρ , ω and their mixing, is described by [35]

$$\begin{aligned}\mathcal{M}_{\gamma^* \rightarrow \pi\pi} &= \mathcal{M}_{\gamma^* \rightarrow \rho I} \frac{1}{s_\rho} \mathcal{M}_{\rho I \rightarrow \pi\pi} \\ &+ \mathcal{M}_{\gamma^* \rightarrow \omega I} \frac{1}{s_\omega} \Pi_{\rho\omega} \frac{1}{s_\rho} \mathcal{M}_{\rho I \rightarrow \pi\pi} \\ &+ \mathcal{M}_{\gamma^* \rightarrow \omega I} \frac{1}{s_\omega} \mathcal{M}_{\omega I \rightarrow \pi\pi}\end{aligned}$$

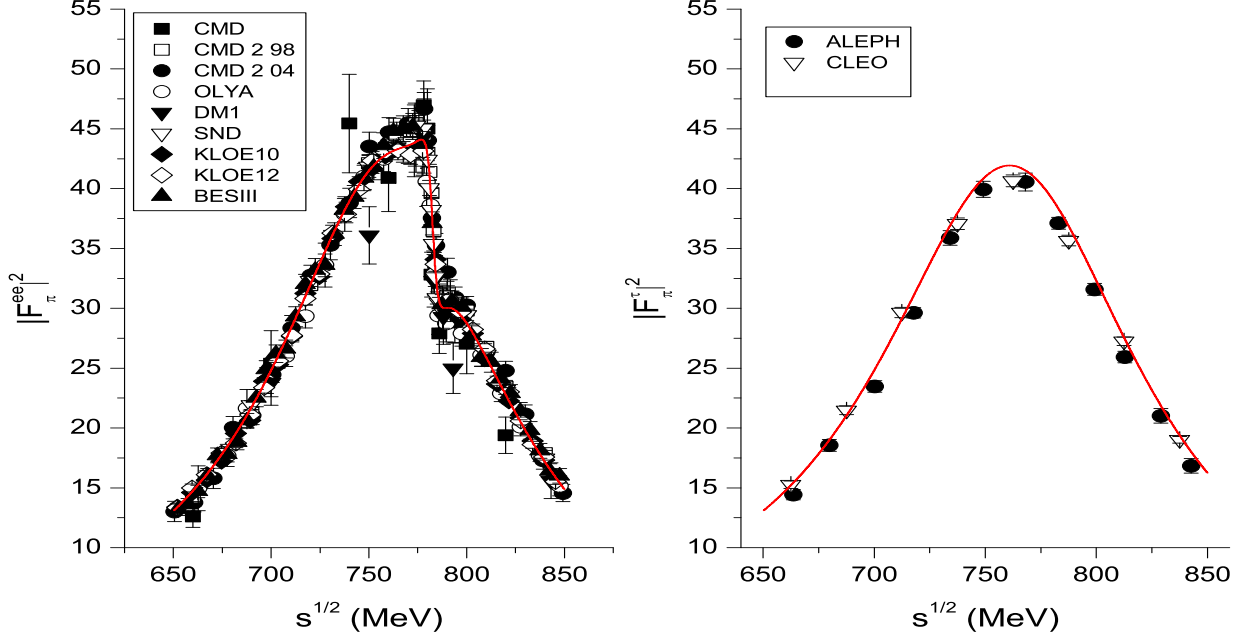


FIG. 2: Fit results for the pion form factor in the $e^+e^- \rightarrow \pi^+\pi^-$ process (left panel) and $\tau \rightarrow \nu_\tau 2\pi$ process (right panel). The data of e^+e^- annihilation are taken from the OLYA and CMD [41], CMD2 [42, 43], DM1 [44], SND [45], KLOE [1, 2], BESIII [3] collaborations. The τ decay data are taken from the ALEPH [46] and CLEO [25] collaborations. The solid lines are our theoretical predictions.

$$+ \mathcal{M}_{\gamma^* \rightarrow \rho I} \frac{1}{s_\rho} \Pi_{\rho\omega} \frac{1}{s_\omega} \mathcal{M}_{\omega I \rightarrow \pi\pi}.$$

Here the fourth term corresponds to higher-order contribution of isospin breaking, e.g., proportional to $(m_u - m_d)^2$, which is beyond our accuracy and hence can be neglected. Including the contribution from the direct coupling of photon to the pion pair, the pion form-factor in e^+e^- annihilation reads

$$F_\pi^{ee}(p^2) = 1 - \frac{G_\rho F_\rho p^2}{F^2} \frac{1}{s_\rho} - \frac{G_\rho F_\omega p^2}{3F^2} \frac{1}{s_\omega} \Pi_{\rho\omega} \frac{1}{s_\rho} - \frac{4\sqrt{2}aB_0 F_\omega (m_u - m_d)p^2}{3F^2} \frac{1}{s_\omega}, \quad (41)$$

On the other hand, the expression of the pion form-factor in $\tau \rightarrow \nu_\tau 2\pi$ decay is

$$F_\pi^\tau(p^2) = 1 - \frac{G_\rho F_\rho p^2}{F^2} \frac{1}{s_\rho}, \quad (42)$$

which is irrelevant to $\rho - \omega$ mixing effect. To take into account the isospin breaking effects, one way is to multiply $|F_\pi^\tau(p^2)|^2$ by the factor of $S_{EW}G_{EM}(s)$, where $S_{EW} = 1.0233$ corresponding to the short distance correction [26]. Furthermore, $G_{EM}(s)$ is responsible for the long distance radiative correction whose expression is provided in [47]. To be specific, in our fit we make the following substitution

$$|F_\pi^\tau(p^2)|^2 \Rightarrow S_{EW}G_{EM}(s)|F_\pi^\tau(p^2)|^2. \quad (43)$$

Our best-fitted parameters and the corresponding $\chi^2/\text{d.o.f.}$ are compiled in Table I. Our determination of the mass of ρ meson is in good agreement with the value reported in PDG [39]. The fit results are plotted in the Fig. 2. One can see that the experimental data of pion form factor, especially the kink around the mass of ω in the $e^+e^- \rightarrow \pi^+\pi^-$ process, is well described.

	Fit results
M_ρ [MeV]	775.3 ± 0.3
G_ρ [MeV]	67.0 ± 3.0
F_ρ [MeV]	152.9 ± 6.8
a [MeV $^{-1}$]	$(-1.8 \pm 0.8) \times 10^{-6}$
X_W^r [MeV $^{-6}$]	$(7.3 \pm 0.2) \times 10^{-17}$
X_Z^r [MeV $^{-4}$]	$(-5.5 \pm 0.6) \times 10^{-11}$
X_R^r [MeV $^{-2}$]	$(-1.1 \pm 0.1) \times 10^{-4}$
f_4^r [MeV 2]	$(1.3 \pm 0.4) \times 10^5$
$\chi^2/\text{d.o.f.}$	$314.9/(242-8)=1.35$

TABLE I: The fit results of the parameters.

In Fig. 3, contributions at different orders to the real and imaginary parts of the pion form factor $F_\pi^{ee}(s)$ are displayed. The leading-order contribution (mixing-effect irrelevant) includes the contact interaction and the ρ -mediated mechanism, namely the first two terms on the right side of Eq. (41). The next-to-leading-order contribution includes the $\rho - \omega$ mixing term and the direct

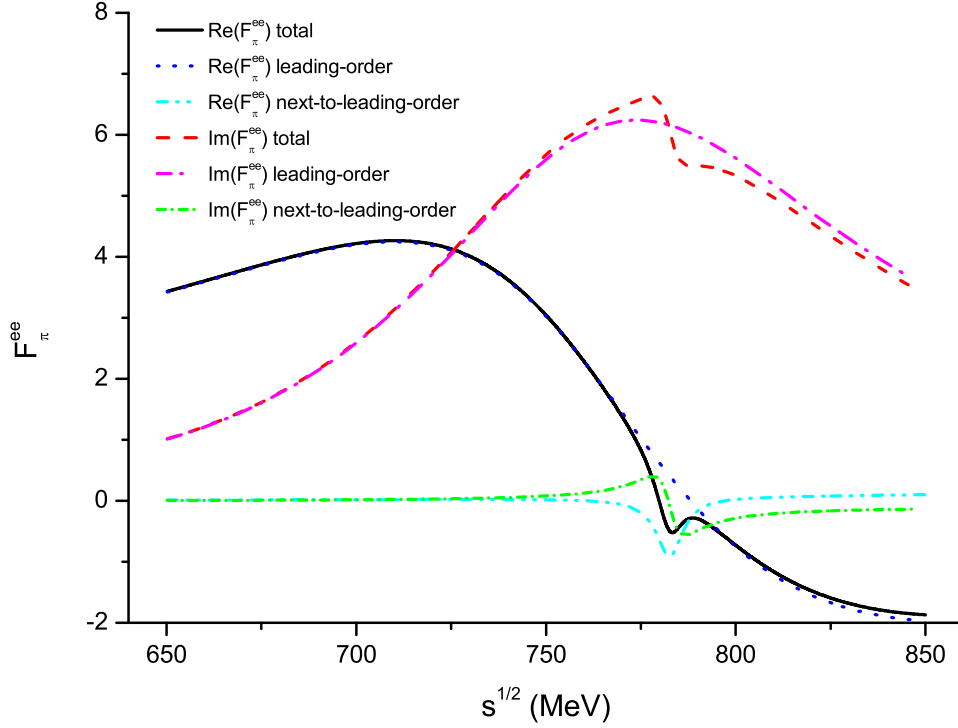


FIG. 3: The real and imaginary parts of the fitted form factor $F_{\pi}^{ee}(s)$. The black solid and red dashed lines represent our best results of the real and imaginary parts, respectively. The blue dotted and cyan dash-dot-dotted lines correspond to the leading order and the second order contributions of the real parts, respectively. The magenta dash-dotted and green short dash-dash-dotted lines denote the leading order and second order contributions of the imaginary parts.

$\omega_I \pi \pi$ coupling, namely the third term plus the fourth term on the right side of Eq. (41). As expected, the isospin-breaking effects mainly affect the energy region around the masses of ρ and ω . It is found that the dominant contribution is from the imaginary part in that region. The isospin-breaking effects increase the absolute value of imaginary part around the ρ peak, and accounts for that the e^+e^- data are higher than the τ data in that region as shown in Fig. 2. Similar behavior has also been observed in Ref. [11] where the $\rho - \omega$ mixing was treated in hidden local symmetry model.

In Fig. 4, we plot the real and imaginary parts of the mixing amplitude $\Pi_{\rho\omega}(s)$. It is found that the real part is dominant almost in all the region and its momentum-dependence is significant. Compared to the real part, the imaginary part is rather small. For the imaginary part, the contributions from $\pi\pi$ loop and $\pi\gamma$ loop are of the same order, but with opposite sign. Note that the π -tadpole is real and s -independent as can be seen from Eq. (25). The smallness of the imaginary part is consistent with the observation in Refs. [5, 48], though therein the effect of direct $\omega_I \rightarrow \pi^+\pi^-$ was not taken into account and even in [5] the isospin breaking is considered to be purely electromagnetic origin. We also note

that larger imaginary part is obtained in [8, 13] by using global color model and a chiral constituent quark model, respectively. However, our finding is more reliable in the sense that it is based on a model-independent description of the $\rho - \omega$ mixing and, moreover, constraint from experimental data is imposed by means of fitting.

The values of $\Pi_{\rho\omega}$ at physical masses of ρ or ω are interesting since they are related to the mixing parameters given in Eq. (6). To that end, we obtain: at $s = M_{\rho}^2$, $\Pi_{\rho\omega}(M_{\rho}^2) = (-2380 - 40.8i) \text{ MeV}^2$ and $\epsilon_2 = 0.21$; at $s = M_{\omega}^2$, $\Pi_{\rho\omega}(M_{\omega}^2) = (-2743.4 - 44.4i) \text{ MeV}^2$ and $\epsilon_1 = 0.24$. As expected, ϵ_1 and ϵ_2 come out to be almost the same. Note that, in the numerical calculation of ϵ_i , we have neglected the small imaginary part of the mixing amplitude as well as the widths of the ρ and ω resonances. This leads to a real number of ϵ_i and hence a probability interpretation can be assigned.

Using the central values of the fitted parameters in Table I, we calculate the decay width of $\omega \rightarrow \pi^+\pi^-$

$$\Gamma_{\omega \rightarrow \pi^+\pi^-} = \frac{1}{192\pi F^4} (M_{\omega}^2 - 4m_{\pi}^2)^{\frac{3}{2}} \left| 8\sqrt{2}B_0(m_u - m_d)a + \frac{2G_{\rho}\Pi_{\rho\omega}(M_{\omega}^2)}{M_{\omega}^2 - M_{\rho}^2 - i(M_{\omega}\Gamma_{\omega} - M_{\rho}\Gamma_{\rho})} \right|^2$$

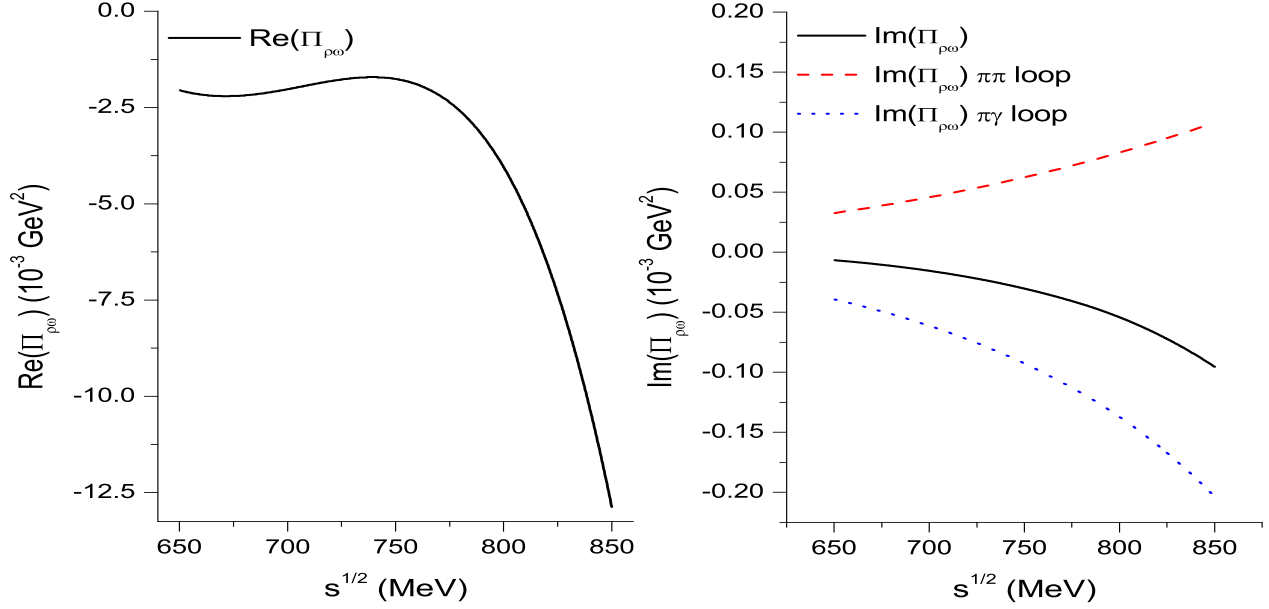


FIG. 4: The real part (left panel) and imaginary part (right panel) of the mixing amplitude $\Pi_{\rho\omega}^{\text{physical}}(s)$. The black solid lines represent our best fitted results. For the imaginary part, the red dashed and blue dotted lines correspond to the contribution of $\pi\pi$ loop and $\pi\gamma$ loop, respectively.

$$= 0.009 | (0.080) + (-0.446 + 3.783i) |^2 \quad (44)$$

From Eq. (44), we can find that the first term due to the direct $\omega_I \rightarrow \pi^+\pi^-$ is less than the second term due to the $\rho - \omega$ mixing by two orders. In other words, the direct $\omega_I \pi^+\pi^-$ coupling only affects the decay width less than one percent. Within 1σ uncertainties, our theoretical value of the branching fraction is $\mathcal{B}(\omega \rightarrow \pi^+\pi^-) = (1.53 \pm 0.10) \times 10^{-2}$, which agrees with the values given in PDG [39] and by the recent dispersive analysis [49].

V. SUMMARY

We have analyzed the $\rho - \omega$ mixing within the framework of resonance chiral theory. Based on the effective Lagrangians constructed under the guidance of various symmetries, we calculate the $\rho - \omega$ mixing amplitude up to next-to-leading order in large $1/N_C$ expansion. Importantly, the momentum-dependent effect is implemented due to the inclusion of loops in our calculation. The values of the resonance couplings are determined by fitting to the data of the pion vector form factor extracted from the $e^+e^- \rightarrow \pi^+\pi^-$ process and $\tau \rightarrow \nu_\tau 2\pi$ decay. The decay width of $\omega \rightarrow \pi^+\pi^-$ is served an additional constraint in the fit as well. It is found that the imaginary part of the pion form factor $F_\pi^{ee}(s)$ is enhanced largely around the ρ peak. The $\rho - \omega$ mixing amplitude is dominated by its real part almost in all the region, which is significantly momentum-dependent. On the contrary, its imaginary part is relatively small. We also find that

$\rho - \omega$ mixing plays a major role in the decay width of $\omega \rightarrow \pi^+\pi^-$, and its contribution is two orders of magnitude larger than that from the direct $\omega_I \pi\pi$ coupling.

Acknowledgments

We would like to thank A. Hosaka and J. J. Sanz-Cillero for helpful discussions. This research is supported in part by the Fundamental Research Funds for the Central Universities under Grant No. 06500077, by the Spanish Ministerio de Economía y Competitividad and the European Regional Development Fund, under contracts FIS2014-51948-C2-1-P, FIS2014-51948-C2-2-P, SEV-2014-0398 and by Generalitat Valenciana under contract PROMETEOII/2014/0068.

-
- [1] KLOE Collaboration, F. Ambrosino *et al.*, Phys. Lett. **B 700**, 102 (2011).
- [2] KLOE Collaboration, D. Babusci *et al.*, Phys. Lett. **B 720**, 336 (2013).
- [3] BESIII Collaboration, M. Ablikim *et al.*, Phys. Lett. **B 753**, 629 (2016).
- [4] S. L. Glashow, Phys. Rev. Lett. **7**, 469 (1961).
- [5] F. M. Renard, Springer Tracts in Modern Physics, **63**, 98C120, Springer-Verlag (1972).
- [6] T. Goldman, J. A. Henderson and A.W.Thomas, Few Body Systems **12** 123C132 (1992).
- [7] C. M. Shakin, W. D. Sun, Phys. Rev. **D 55**, (1997) 2874.
- [8] K. L. Mitchell and P. C. Tandy, Phys. Rev. **c 55**, (1997) 1477.
- [9] M. Benayoun *et al.*, Eur. Phys. J. **C 17**, 303C321 (2000).
- [10] M. Benayoun *et al.*, Eur.Phys.J. **C 22**, 503-520 (2001).
- [11] M. Benayoun *et al.*, Eur. Phys. J. **C 55**, 199C236 (2008).
- [12] D. N. Gao, M. L. Yan, Eur. Phys. J. **A 3**, 293-298 (1998).
- [13] X. J. Wang, M. L. Yan, Phys. Rev. **D 62**, (2000) 094013.
- [14] G. Ecker, J. Gasser, A. Pich and E. de Rafael, Nucl. Phys. **B321** (1989) 311.
- [15] Z. H. Guo and J. A. Oller, Phys. Rev. D **84**, 034005 (2011).
- [16] M. Jamin, A. Pich, and J. Portoles, Phys. Lett. **B 640**, 176 (2006).
- [17] P. Roig and J. J. Sanz-Cillero, Phys. Lett. B **733** (2014) 158.
- [18] Y. H. Chen, Z. H. Guo, H. Q. Zheng, Phys. Rev. D **85**, 054018 (2012).
- [19] Y. H. Chen, Z. H. Guo, H. Q. Zheng, Phys. Rev. D **90**, 034013 (2014).
- [20] Y. H. Chen, Z. H. Guo and B. S. Zou, Phys. Rev. D **91**, 014010 (2015).
- [21] Res Urech, Phys. Lett. **B 355** (1995) 308.
- [22] A. Kucukarslan, Ulf-G. Meißner, Mod. Revs. Lett. **A 21**, 1423 (2006).
- [23] G. t'Hooft, Nucl. Phys. **B72** (1974); **75** (1974) 461.
- [24] I. Rosell, J. J.Sanz-Cillero and A. Pich, JHEP **0408** (2004) 042.
- [25] CLEO Collaboration, S. Anderson *et al.*, Phys. Rev. **D 61**, 112002 (2000).
- [26] M. Davier, *et al.*, Eur. Phys. J. **C 27** (2003) 497.
- [27] R. Alemany, *et al.*, Eur. Phys. J. **C 2** (1998) 123.
- [28] J. A. Oller, E. Oset and J. E. Palomar, Phys. Rev. D **63**, 114009 (2001).
- [29] V. Cirigliano, *et al.*, Phys. Lett. **B 513**, 361 (2001).
- [30] V. Cirigliano, *et al.*, Eur. Phys. J. **C 23** (2002) 121.
- [31] S. Ghoszi, F. Jegerlehner, Phys. Lett. **B 583**, 222 (2004).
- [32] K. Maltman, C.E.Wolfe, Phys. Rev. **D 73**, 013004 (2006).
- [33] L. Y. Dai, J. Portoles and O. Shekhovtsova, Phys. Rev. D **88**, 056001 (2013).
- [34] D. Djukanovic, J. Gegelia, A. Keller, S. Scherer and L. Tiator, Phys. Lett. B **742**, 55 (2015).
- [35] H. B. O'Connell, B.C. Pearce, A. W. Thomas and A. G. Williams, Prog. Nucl. Part. Phys. **39** (1997) 201-252.
- [36] J. Gasser and H. Leutwyler, Annals Phys. **158**, 142 (1984); J. Gasser and H. Leutwyler, Nucl. Phys. **B250**, 465 (1985).
- [37] P. D. Ruiz-Femenia, A. Pich, J. Portoles, JHEP **0307** (2003) 003.
- [38] V. Mateu and J. Portoles, Eur. Phys. J. **C 52**, 325 (2007).
- [39] C. Patrignani *et al.* [Particle Data Group Collaboration], Chin. Phys. C **40**, 100001 (2016).
- [40] D. Gomez-Dumm, A. Pich, and J. Portoles, Phys. Rev. **D 62**, (2000) 054014.
- [41] L. M. Barkov *et al.*, Nucl. Phys. **B 256**, 365 (1985).
- [42] CMD-2 Collaboration, R. R. Akhmetshin *et al.*, Phys. Lett. **B 578**, 285 (2004).
- [43] CMD-2 Collaboration, R. R. Akhmetshin *et al.*, JETP Lett. **84**, 413 (2006).
- [44] A. Quenzer *et al.*, Phys. Lett. **B 76**, 512 (1978).
- [45] M. N. Achasov *et al.*, J. Exp. Theor. Phys. **103**, 380 (2006).
- [46] ALEPH Collaboration, S. Schael *et al.*, Phys. Rep. **421**, 191 (2005).
- [47] F. Flores-Baez *et al.*, Phys. Rev. **D 74**, (2006) 071301.
- [48] S. Gardner and H. B. O'Connell, Phys. Rev. **D 57**, (1998) 2716.
- [49] C. Hanhart, S. Holz, B. Kubis, A. Kupsc, A. Wirzba and C. W. Xiao, Eur. Phys. J. **C 77** (2017) 98.